JOURNAL OF GUIDANCE, CONTROL, AND DYNAMICS
Vol. 22, No. 6, November–December 1999

Regulation About Time-Varying Trajectories: Precision Entry Guidance Illustrated

Ping Lu*
Iowa State University, Ames, Iowa 50011-3231

A new method for regulating nonlinear dynamic systems about time-varying reference trajectories is introduced. The control law is a closed-form approximate receding-horizon control law based on the linearized time-varying dynamics. No on-line integration or explicit gain scheduling is required for implementation. Closed-loop stability can always be achieved with such a control law. The application of this method in entry guidance for the X-33 vehicle leads to very accurately controlled flight in all the state variables in simulations, which was difficult to achieve previously. This application demonstrates the potential of this approach as a powerful guidance and trajectory control method in cases for which high precision is required.

I. Introduction

THE trajectory control problem for dynamic systems is often addressed in two steps: off-line trajectory planning and on-line trajectory tracking. It is the case for many robot control problems. In aerospace engineering, entry guidance of a spacecraft is currently performed this way. Off-line trajectory planning allows careful design of the trajectory to satisfy all the constraints, optimize performance, and balance the conflicting requirements arising from different aspects of the mission. In the on-line implementation, however, some judicious choices in deciding how to accomplish the control objectives may have to be made because of the limited number of controls and nonlinear dynamics. For instance, in the entry guidance problem, the primary means for trajectory control is through modulation of the bank angle. Current nonlinear control methodology does not render a practical solution to tracking the three-dimensional reference trajectory in the state space (six state variables). The Space Shuttle and the X-33 entry guidance systems opt to track a nominal drag profile derived from the reference trajectory for the downrange control, and the crossrange control is achieved by reversing the sign of the bank angle when certain heading error threshold criteria are exceeded.[1–3] Although the downrange distance and energy can be accurately controlled in this way, a different guidance strategy may have to be used near the end if additional requirements on other state variables such as the heading angle need to be met, as in the case of the X-33 (Refs. 2–4). The use of another guidance strategy, however, may in turn interfere with accurately achieving the end conditions in position and altitude.

An alternative is to treat the trajectory tracking problem as a regulation problem in the state space about the reference trajectory. If effective control laws based on the linearized dynamics can be developed to null the deviations from the reference trajectory, this approach should be quite appealing because the reference trajectory has already been designed to meet all the mission requirements. One major stumbling block to this approach has been due to the fact that the linearized system is time varying because of the time-varying nature of the reference trajectory. In a sharp contrast to the extensive body of design methods for linear time-invariant systems, there have been relatively very few available methods for controller design to stabilize a linear time-varying (LTV) system. A commonly used technique is to design the controller at a number of points along the trajectory, and then interpolate the gains over the flight envelope. Reference 5 presents such an application for entry trajectory control. The practical disadvantages of this technique are that the point designs of the controller and gain scheduling are manpower intensive and highly time consuming, and the entire process has to be repeated for each different reference trajectory for different missions. On an equally (if not more) important note, a fundamental issue is that stability cannot be theoretically guaranteed by such a gain-scheduled controller. Therefore extensive simulations are usually required for verifying the control law, which further adds to the mission costs.

In a recent work,[6] a closed-form stabilizing control law for LTV systems has been developed. The control law is based on an approximation to the solution of a receding-horizon control problem. Once the control law is developed, no on-line integrations or explicit gain scheduling are required, and the control law has the same form for different reference trajectories. A stabilizing control law can always be constructed in this way to guarantee the closed-loop stability of the linearized, time-varying system, and hence the stability of the original nonlinear system in a neighborhood of the reference trajectory.

In this paper, this control design method is introduced as a potentially powerful trajectory control tool for nonlinear systems. The problem of entry guidance for the X-33 Advanced Technology Demonstrator is revisited with this method. The simulations demonstrate tight regulation of all the state variables for the three-dimensional motion in the presence of relatively large trajectory dispersions. All the conditions at the terminal area energy management (TAEM) interface (the end of entry flight) match the nominal ones very well, which previous studies[2–4] have not been able to achieve.

II. Stabilizing Control Laws for Linear Time-Varying Systems

The development of the control laws is briefly outlined here for completeness and the convenience of the reader. For more technical details, the reader is referred to Ref. 6. Consider an LTV system

$$\dot{x} = A(t)x + B(t)u \tag{1}$$

where $x \in R^n$, $u \in R^m$, and $A(\cdot) : R \to R^{n \times n}$ and $B(\cdot) : R \to R^{n \times m}$ are continuous. System (1) is assumed to be uniformly completely controllable.[7] A control law $u = K(t)x$ is sought to stabilize system (1) at the origin for any initial condition $x(t_0)$.

Receding-Horizon Control Problem

The receding-horizon control approach is one of the few existing methods for LTV systems. The receding-horizon control problem at any $t \geq t_0$ is defined to be an optimal control problem in which the performance index

$$J = \int_t^{t+T} [x^T(\tau)Qx(\tau) + u^T(\tau)Ru(\tau)]\,\mathrm{d}\tau \tag{2}$$

Received 20 November 1998; revision received 10 May 1999; accepted for publication 10 May 1999.

*Associate Professor, 498 Town Engineering Building, Department of Aerospace Engineering and Engineering Mechanics; plu@iastate.edu. Associate Fellow AIAA.

is minimized for some $Q \geq 0$ and $R > 0$, subject to system dynamics (1), initial condition $x(t)$, and the terminal constraint

$$x(t+T) = 0 \tag{3}$$

with $\delta_c \leq T < \infty$, where $\delta_c > 0$ is a constant used in the definition of uniform controllability of system (1) (Ref. 7). The idea is to solve this optimal control problem in the finite moving horizon $[t, t+T]$ with the current state $x(t)$ as the initial condition. Let $u_{\text{optm}}(\cdot)$ be the optimal control obtained in $[t, t+T]$. Only the first data $u_{\text{optm}}(t)$ are used to be the current applied control $u(t) = u_{\text{optm}}(t)$. The rest of $u_{\text{optm}}(\cdot)$ is discarded. The process is then repeated for the next t. Thus the receding-horizon control strategy is different from applying $u(\tau) = u_{\text{optm}}(\tau)$ for all $\tau \in [t, t+T]$.

Kwon and Pearson[8] show that the receding-horizon control strategy for any fixed $T \in [\delta_c, \infty)$ gives the control

$$u^*(t) = -R^{-1}B^T(t)P^{-1}(t, t+T)x(t) \triangleq K^*(t)x(t) \tag{4}$$

where $P(t_1, t_2) > 0$ satisfies the matrix Riccati differential equation at any $\tau \in [t, t+T] \triangleq [t, t_T]$:

$$-\frac{\partial P(\tau, t_T)}{\partial \tau} = -A(\tau)P(\tau, t_T) - P(\tau, t_T)A^T(\tau) - P(\tau, t_T)QP(\tau, t_T) + B(\tau)R^{-1}B^T(\tau) \tag{5}$$

with the boundary condition

$$P(t_T, t_T) = P(t+T, t+T) = 0 \tag{6}$$

To compute $u^*(t)$ from Eq. (4), Riccati equation (5) needs to be integrated backward from $t+T$ to t with boundary condition (6). The closed-loop system under control law (4) is uniformly asymptotically stable, provided system (1) is uniformly controllable.[8]

Approximate Receding-Horizon Control Law

The need for backward integration of matrix Riccati differential equation (5) at every instant t poses a serious computational burden for on-line implementation of control law (4). An analytical approximation to control law (4) is developed in Ref. 6 as follows: Consider the preceding receding-horizon problem in the interval $[t, t+T]$. Divide this interval into N subintervals of equal length $h = T/N$ for some integer $N \geq n/m$. With the current state $x(t)$ known, a first-order prediction of $x(t+h)$ as a function of $u(t)$ is given by a Taylor series expansion at t:

$$x(t+h) \approx x(t) + h[A(t)x(t) + B(t)u(t)] = (I + hA)x + hBu \tag{7}$$

Denote $A_k = A(t+kh)$, $B_k = B(t+kh)$, $x_k = x(t+kh)$, and $u_k = u(t+kh)$, $k = 1, \ldots, N$. Then another first-order Taylor series expansion at $t+h$, together with approximation (7), gives

$$x(t+2h) \approx x_1 + h(A_1x_1 + B_1u_1) \approx (I + hA_1)(I + hA)x + h(I + hA_1)Bu + hB_1u_1 \tag{8}$$

Continuing this process, we have

$$x_k \approx \Delta_k x + \sum_{i=0}^{k-1} G_{k,i}u_i, \qquad k = 1, \ldots, N \tag{9}$$

where

$$\Delta_k = (I + hA_{k-1})\Delta_{k-1}, \quad \text{with} \quad \Delta_0 = I \tag{10}$$

$$G_{k,i} = (I + hA_{k-1})G_{k-1,i}, \qquad i = 0, 1, \ldots, k-2$$

$$G_{k,k-1} = hB_{k-1} \tag{11}$$

The subscript 0 in the preceding expressions denotes the values at t. Let $L_0 = x^T(t)Qx(t) + u^T(t)Ru(t)$ and $L_k = x_k^T Qx_k + u_k^T Ru_k$, $k = 1, \ldots, N$. The integral in Eq. (2) is approximated by the standard trapezoidal formula for integrals:

$$J \approx h(0.5L_0 + L_1 + \cdots + L_{N-1} + 0.5L_N) \tag{12}$$

Define an (mN)-dimensional vector $\boldsymbol{v} = \text{col}\{u(t), u_1, \ldots, u_{N-1}\}$. If the x_k in Eq. (12) are replaced with prediction (9), the performance index is thus approximated by a quadratic function of $\boldsymbol{v}$:

$$\bar{J} = \tfrac{1}{2}\boldsymbol{v}^T H(t, N, h)\boldsymbol{v} + x^T S(t, N, h)\boldsymbol{v} + q(x, t, N, h, u_N) \tag{13}$$

where $H \in R^{mN \times mN}$ is positive definite for any $t \geq t_0$, integer N and $h > 0$; $S \in R^{n \times mN}$; and q is quadratic in x and u_N. These terms are obtained directly by rearranging the expression of J in formula (12) once the x_k are replaced with prediction (9). The Appendix gives the expressions of H and S for $N = 2$, 3, and 4. Constraint (3) can be approximated by setting $x_N = 0$ from prediction (9), which can be rewritten in a compact form:

$$M^T(t, N, h)v = -\Delta_N x \tag{14}$$

where

$$M^T = [G_{N,0} \cdots G_{N,N-1}] \in R^{n \times mN} \tag{15}$$

The minimization of $\bar{J}$ in Eq. (13) with respect to $\boldsymbol{v}$ subject to constraint (14) constitutes a quadratic programming (QP) problem. It is shown in Ref. 6 that for sufficiently small h (equivalently, sufficiently large N for a fixed T), M^T has full rank, given the uniform controllability of the system. Then the preceding QP problem has a unique solution:

$$\boldsymbol{v} = -\left\{\left[H^{-1} - H^{-1}M(M^T H^{-1}M)^{-1}M^T H^{-1}\right]S^T + \left[H^{-1}M(M^T H^{-1}M)^{-1}\right]\Delta_N\right\}x \tag{16}$$

Define an $m \times mN$ matrix:

$$I_{mN} = \{I_{m \times m}, 0, \ldots, 0\} \tag{17}$$

A closed-form, LTV feedback control law for $u(t)$, denoted by $\bar{u}(t; N, h)$ hereafter to signify its dependence on time and the values of N and h, is then obtained from the first m equations in Eq. (16):

$$\bar{u}(t; N, h) = I_{mN}v \triangleq K(t, N, h)x(t) \tag{18}$$

It should be noted at this point that for different values of N, the expression of the gain $K(t, N, h)$ in the control law $\bar{u}(t; N, h)$ will be different. The functional form of $K(t, N, h)$ does not change with the value of h for the same N, but the values of the gain $K(t, N, h)$ do vary with different h. For a fixed N, smaller h normally means higher controller gains. It is shown in Ref. 6 that the difference between control $\bar{u}(t; h)$ and $u^*(t)$ in Eq. (4) at the same t is proportional to h. The analysis in Ref. 6 further proves that if $A(t)$ and $B(t)$ are bounded with respect to t, for a fixed T, there exists an $h^* > 0$ such that for all $N \geq T/h^*$ and $h = T/N \leq h^*$, the closed-loop system under control $\bar{u}(t; h)$ is uniformly asymptotically stable; Or, equivalently, for a sufficiently large N, the closed-loop stability is ensured with $h = T/N$. Note that the expression of control law (18) [the gain $K(t, N, h)$ in specific] would be different for different values of N. The proof of stability is based on the recognition that prediction (9) is in fact the Euler integration algorithm applied to system (1) and trapezoidal formula (12) is a second-order approximation to the integral in Eq. (2). The stability conclusion is then obtained from the application of Lyapunov stability theory to the LTV system.

Higher-order approximate receding-horizon control laws are also discussed in Ref. 6 when higher-order expansions for $x(t+kh)$ and higher-order quadrature formulas for the performance integral of Eq. (2) are used. But for our subsequent entry guidance application no clear advantages seem to be gained with higher-order control laws. Therefore we concentrate on first-order control law (18).

It may be useful to reiterate that the development of control law (18) is a one-time effort. No explicit gain scheduling or on-line integrations is needed in implementation once system model (1) is known. The determination of appropriate values of N and h for a specific system is typically not difficult simply by trial. In all the tests conducted, it was found that the value of N need not be very large (alternatively, the value of h need not be very small for fixed T) to achieve closed-loop stability. In most cases it appears that a value of $N \approx n/m$ suffices (where n is the number of

state variables). On the other hand, the parameter h is inversely proportional to the controller gain. For a given N, smaller h produces a faster response with larger control and possibly large overshoot, and vice versa. Once the value of N is determined, it is more convenient to treat and adjust h as a controller gain parameter rather than fix on its time-step interpretation used in the control law derivation.

Proportional-plus-Integral Control Law

Although Eq. (18) gives a time-varying proportional feedback control law, in certain cases a proportional-plus-integral (PI) control law may be desired for better steady-state performance and robustness in the presence of modeling uncertainty and disturbances. Although the development in Ref. 6 does not explicitly address this possibility, the approach can be readily extended to construct a PI controller for LTV systems.

Suppose that, in addition to system model (1), there are some functions of interest defined by

$$y = C(t)x \tag{19}$$

where $y \in R^p$ and $C : R \to R^{p\times n}$ is continuous and bounded with respect to t. When tight regulation of y is particularly required, the control law may be desired to contain a term proportional to the integral of y. To this end, a new quantity is introduced:

$$z(t) = \int_{t_0}^{t} y(\tau)\,\mathrm{d}\tau \tag{20}$$

Define an augmented system:

$$\dot{w} = \begin{bmatrix}\dot{x}\\ \dot{z}\end{bmatrix} = \begin{bmatrix}A(t) & 0\\ C(t) & 0\end{bmatrix}\begin{bmatrix}x\\ z\end{bmatrix} + \begin{bmatrix}B(t)\\ 0\end{bmatrix}u \triangleq \tilde{A}(t)w + \tilde{B}(t)u \tag{21}$$

Now if augmented LTV system (21) is uniformly controllable, the approach in the preceding section can be taken to derive a closed-form approximate receding-horizon control law for system (21):

$$u(t) = K_w(t, N, h)w = K_1(t, N, h)x + K_2(t, N, h)z$$

$$= K_1(t, N, h)x + K_2(t, N, h)\int_{t_0}^{t} y(\tau)\,\mathrm{d}\tau \tag{22}$$

This is a PI control law to original system (1). A stability discussion similar to the one in the preceding section applies to system (21).

III. Entry Guidance for the X-33 Vehicle

The X-33 Advanced Technology Demonstrator is a half-scale prototype for a reusable launch vehicle (RLV). The primary technical goals of the X-33 program are to develop and test key technologies needed for the next-generation single-stage-to-orbit RLV. Figure 1 shows the configuration of the X-33. The X-33 will be launched vertically from Edwards Air Force Base, California, and land horizontally at Michael Army Air Field (AAF) in Utah. The flight trajectories will cover a range of Mach numbers for various test objectives such as maximum entry catalytic heating, maximum entry integrated heat load, and maximum delay of transition to turbulent flow.

After a short transition phase following the main engine cutoff at an altitude of approximately 56 km, the X-33 is guided by the entry guidance system toward the landing site until it reaches the TAEM interface, which is at Mach 3 and 55 km from the heading alignment cylinder (HAC). Thus a major portion of the flight is under the control of the entry guidance system. The effectiveness and the accuracy of the entry guidance scheme are key factors in ensuring the success of the flight tests. The principle of the entry guidance for the X-33 is similar to that of the Space Shuttle with incorporation of many recent developments in aerospace guidance and control research. A 3-degree-of-freedom (DOF) reference trajectory is first generated by trajectory optimization methods. The nominal drag acceleration profile is extracted from the 3-DOF trajectory and used on board as the reference. The magnitude of the bank angle is modulated to track the reference drag profile, and the sign of the bank angle is used to control the crossrange motion through bank reversals.[2–4]

Although this guidance strategy works well for most of the entry flight, it was found that bank reversals have difficulty in providing tight control of the velocity azimuth angle to meet the required heading conditions at the TAEM interface, especially when the bank rate is constrained. Therefore the guidance strategy switches to a different heading alignment logic before the X-33 arrives at the TAEM interface.[2–4] But this guidance logic that emphasizes heading control tends to produce too high an altitude and too shallow a trajectory at the TAEM interface.[2–4] Further additional compensations have to be made for these undesirable effects.[4] The trajectory-regulation method introduced in the preceding section provides a uniform approach for addressing the needs of controlling the trajectory to meet these competing requirements. Here the entry guidance problem for the X-33 is revisited and the potential of the current approach is demonstrated.

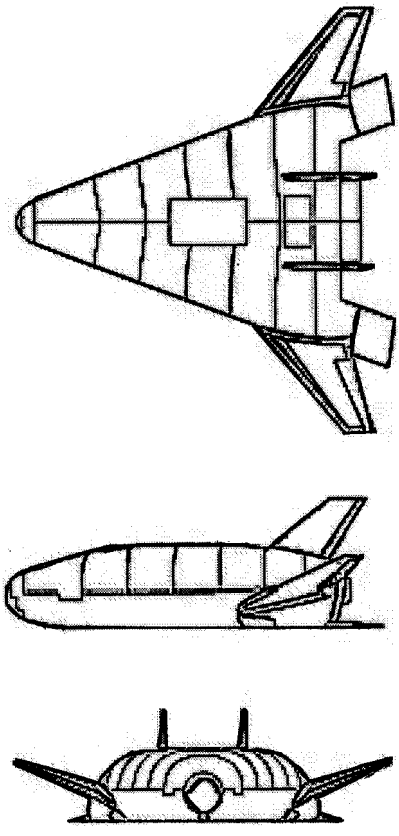

Fig. 1 X-33 Advanced Technology Demonstrator.

Reference Trajectory

To apply the trajectory-regulation method to entry guidance of the X-33, we first generate a reference trajectory. We begin with the point-mass dimensionless equations of three-dimensional motion over a spherical, rotating Earth[9]:

$$\dot{r} = V\sin\gamma \tag{23}$$

$$\dot{\theta} = \frac{V\cos\gamma\sin\psi}{r\cos\phi} \tag{24}$$

$$\dot{\phi} = V\cos\gamma\cos\psi/r \tag{25}$$

$$\dot{V} = -D - \sin\gamma/r^2 + \Omega^2 r\cos\phi(\sin\gamma\cos\phi - \cos\gamma\sin\phi\cos\psi) \tag{26}$$

$$\dot{\gamma} = (1/V)[L\cos\sigma + (V^2 - 1/r)(\cos\gamma/r) + 2\Omega V\cos\phi\sin\psi + \Omega^2 r\cos\phi(\cos\gamma\cos\phi + \sin\gamma\cos\psi\sin\phi)] \tag{27}$$

$$\dot{\psi} = (1/V)[L\sin\sigma/\cos\gamma + (V^2/r)\cos\gamma\sin\psi\tan\phi - 2\Omega V(\tan\gamma\cos\psi\cos\phi - \sin\phi) + (\Omega^2 r/\cos\gamma)\sin\psi\sin\phi\cos\phi] \tag{28}$$

where r is the radial distance from the center of the Earth to the X-33, normalized by the radius of the Earth $R_0 = 6378$ km. The longitude and the latitude are θ and ϕ, respectively. The Earth's relative velocity V is normalized by $\sqrt{(g_0 R_0)}$ with $g_0 = 9.81$ m/s^2. D and L are aerodynamic accelerations in g's. Ω is the rotation rate of the Earth normalized by $\sqrt{(g_0/R_0)}$. γ is the flight-path angle, and σ is the bank angle. The velocity azimuth angle ψ is measured from the north in a clockwise direction. The differentiation is with respect to the dimensionless time $\tau = t/\sqrt{(R_0/g_0)}$.

The initial conditions for the entry trajectory are chosen to be a Mach 10 trajectory beginning at an altitude of 55 km and 435 km away from the TAEM interface near Michael AAF. The TAEM conditions are specified according to early X-33 trajectory data, in terms of altitude (25 km), Mach number (2.5), velocity azimuth, longitude, and latitude. In addition, the following trajectory constraints are imposed:

$$|L\cos\alpha + D\sin\alpha| \le n_{z_{\max}} \tag{29}$$

$$\bar{q} \le \bar{q}_{\max} \tag{30}$$

$$\dot{Q}_s \le \dot{Q}_{\max} \tag{31}$$

where relation (29) is a constraint on the acceleration in the body-normal direction, relation (30) is a constraint on dynamic pressure $\bar{q}$, and relation (31) is a constraint on heat rate $\dot{Q}_s$ at a stagnation point. Multiple heat rate constraints for several stagnation points can be imposed, although only one is used here. In this study, $n_{z_{\max}} = 2.5$ (g), $\bar{q}_{\max} = 11{,}970$ N/m^2 (250 psf), and $\dot{Q}_{\max} = 431{,}259$ W/m^2 (38 Btu/s $\cdot$ ft^2) are used.

In the design of the nominal entry trajectory, the angle of attack α is scheduled as a function of Mach number, beginning at a large value (45 deg) and gradually reducing to 15 deg at the TAEM point. The bank angle σ is parameterized by cubic spline functions of time. The nodal values of the parameterization of σ and the flight time τ_f are treated as the parameters to be determined. A feasible trajectory satisfying all the TAEM conditions and in-flight constraints (29–31) is found by a sequential quadratic programming algorithm[10] that determines the values of those parameters. The X-33 basic vehicle aerodynamic data are used, and the models for atmospheric density and speed of sound are based on the 1976 U.S. standard atmosphere. Figures 2–4 show the variations of the six state variables, bank angle,

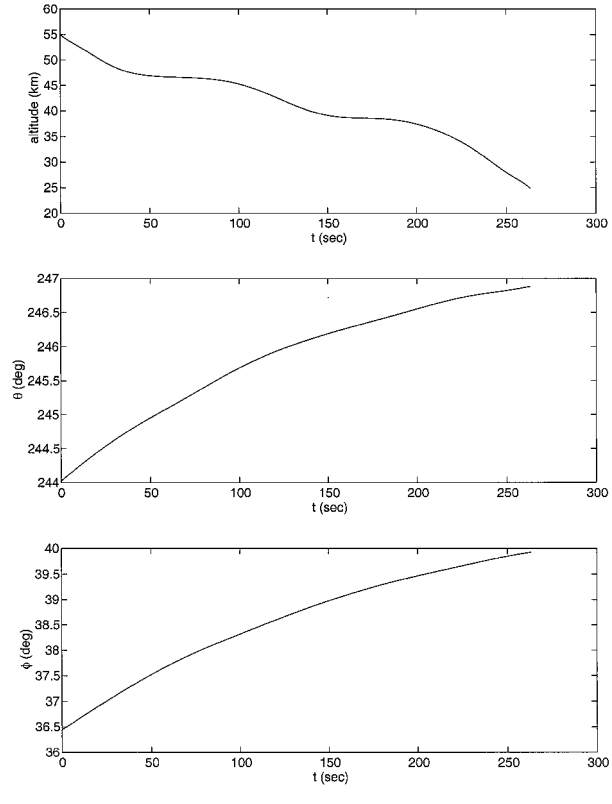

Fig. 2 Variations of nominal altitude, longitude θ, and latitude ϕ.

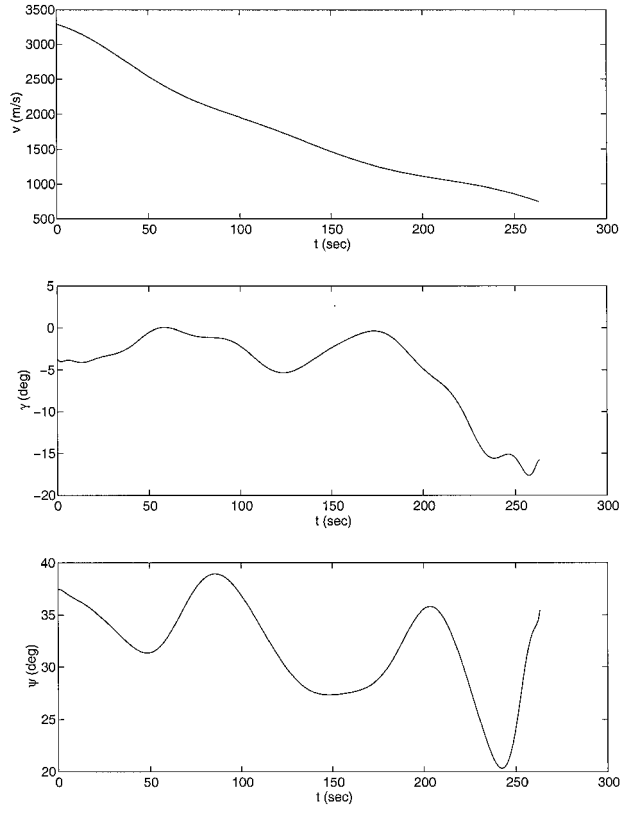

Fig. 3 Variations of nominal velocity v, flight-path angle γ, and heading angle ψ.

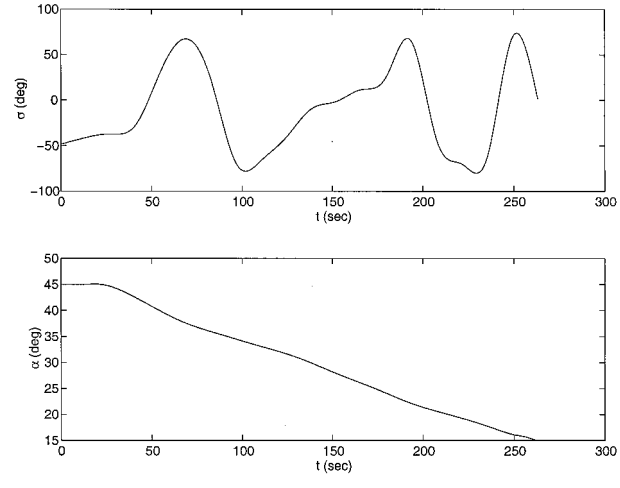

Fig. 4 Variations of nominal bank angle σ and angle of attack α.

and α along the reference trajectory. They are clearly very much time varying in nature.

Closed-Loop Guidance by Trajectory Regulation

Let $x = (r\theta\phi V\gamma\psi)^T$ and $u = (\sigma\alpha)^T$. We allow some feedback modulation of α for better trajectory control as it is done in Space Shuttle and X-33 entry guidance.[1,2] Let $\Delta x(\tau)$ and $\Delta u(\tau)$ denote the differences between the actual and the nominal values in x and u. The linearized dynamics of system (23–28) about the reference trajectory are

$$\Delta\dot{x} = A(\tau)\Delta x + B(\tau)\Delta u \tag{32}$$

With the tabulated data for the lift and drag coefficients of the basic X-33 vehicle fitted by bivariate rational functions of α and Mach number, the expressions of the elements in the Jacobian matrices

A and B are obtained analytically from Eqs. (24–28). Their values at each τ depend on the state and control histories of the reference trajectory. Applying control law (18) to system (32), we have a feedback control law for $\Delta u = K(\tau)\Delta x$, where K is dependent on $A(\tau)$, $B(\tau)$, N, and h. The actual trajectory is then controlled by $u(\tau) = u^*(\tau) + \Delta u(\tau)$ with the nonlinear dynamics governed by system (23–28), where the asterisk denotes the reference value. In other words, in the subsequent simulations, Δx is not generated from linearized system (32), but from $\Delta x(\tau) = x(\tau) - x^*(\tau)$, where $x(\tau)$ is the state response from system (23–28) with $u(\tau) = u^*(\tau) + \Delta u(\tau)$. Linearized model (32) is used only for the control law construction for Δu. Successful trajectory regulation should lead to $\Delta x \to 0$, and thus $\Delta u \to 0$, provided the trajectory dispersions are not so large as to invalidate the linearization approximation or cause destabilizing control saturation.

For system (32), $n = 6$ and $m = 2$. The parameter N in control law (18) must be at least greater than $n/m = 3$. It was found that any $N \geq 4$ for this application suffices to yield a satisfactory stabilizing control law for Δu. The control law is too lengthy to present here, but otherwise a straightforward matter to obtain by following the systematic formulas given in Sec. II. Coding of the control law with existing control system software packages such as MATLAB® is particularly easy. All the reference state histories are fitted by rational functions or polynomials to reduce data storage and interpolation needs. Commercial software is available to perform the curve fitting efficiently and to generate computer codes for the fittings. For different reference trajectories, the control law code remains the same, and the only changes will be in the curve fittings for the reference trajectory.

To assess the effectiveness of this guidance method under diverse conditions, we let the trajectory dispersions at the starting point be randomly distributed in the ranges of

$$|\Delta r(0)| \leq 3 \text{ (km)}, \qquad |\Delta\theta(0)| \leq 0.05 \text{ (deg)}$$
$$|\Delta\phi(0)| \leq 0.05 \text{ (deg)}, \qquad |\Delta V(0)| \leq 150 \text{ (m/s)}$$
$$|\Delta\gamma(0)| \leq 2 \text{ (deg)}, \qquad |\Delta\psi(0)| \leq 5 \text{ (deg)} \tag{33}$$

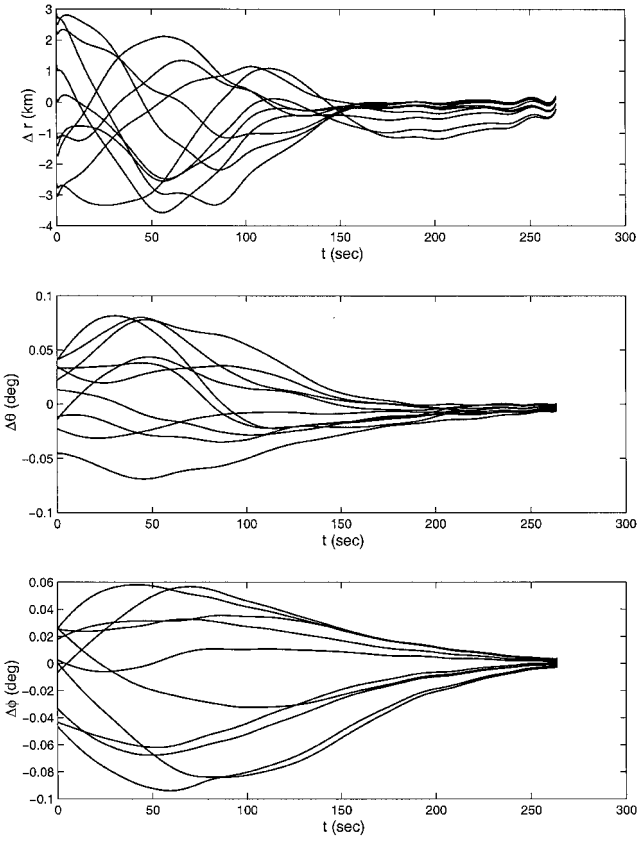

Fig. 5 Dispersions in altitude, longitude, and latitude.

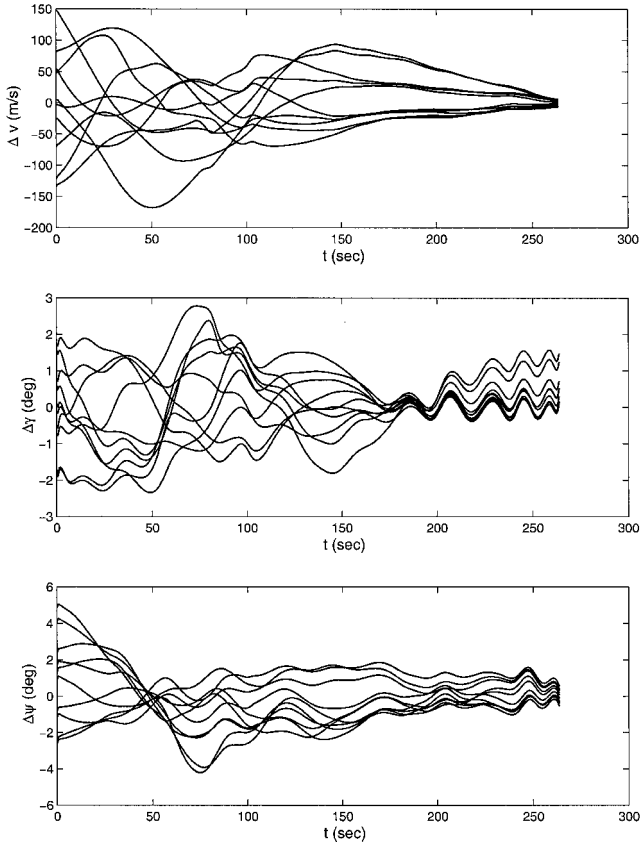

Fig. 6 Dispersions in velocity, flight-path angle, and heading angle.

These represent significant dispersions for entry flight of the X-33. The reference trajectory in Figs. 2–4 is the nominal. For the trajectory control law used in the simulations described in this paper, $N = 7$, $h = 0.02$ (dimensionless, 16 s in real time), Q is the unity matrix, and $R = \text{diag}\{5,\ 0.01\}$ (with σ in radians and α in degrees) are used. The sizes of $\Delta\sigma$ and $\Delta\alpha$ are bounded by the conditions

$$|\sigma^*(\tau) + \Delta\sigma(\tau)| \leq 90 \text{ (deg)} \tag{34}$$

$$|\Delta\alpha(\tau)| \leq \Delta\alpha_{\max}(\tau) \tag{35}$$

where $\Delta\alpha_{\max}$ is scheduled with respect to Mach number, starting at 5 deg at Mach 10 and linearly increasing to 10 deg at Mach 2.5.

Many trajectories have been simulated with initial conditions randomly perturbed away from the reference in the ranges specified in relations (33). Figures 5 and 6 depict the variations of the trajectory dispersions along 10 such trajectories. At the TAEM interface along all the 10 trajectories, the altitude errors are less than 0.3 km, the circular position errors less than 0.65 km, the velocity errors less than 7 m/s, the flight-path angle errors less than 1.5 deg, and the heading angle errors less than 0.6 deg. This level of accuracy represents a major improvement in the precision that trajectory control can achieve in the context of entry guidance. It would already be difficult for the methods in previous works[2–4] to attain similar accuracy in just a few of the state variables in a dispersion study, let alone the level of overall precision demonstrated here. It should be noted that no navigation uncertainty is considered in the preceding assessment.

The variations of complete σ and α (not just dispersions) along those 10 trajectories are shown in Fig. 7. It can be seen that as the trajectory dispersions are reduced by the feedback control law, the bank angle and the angle of attack return to their nominal values.

Discussion

1) Although the independent variable used in the preceding discussion is the time, it is not a necessity. In fact, if the use of

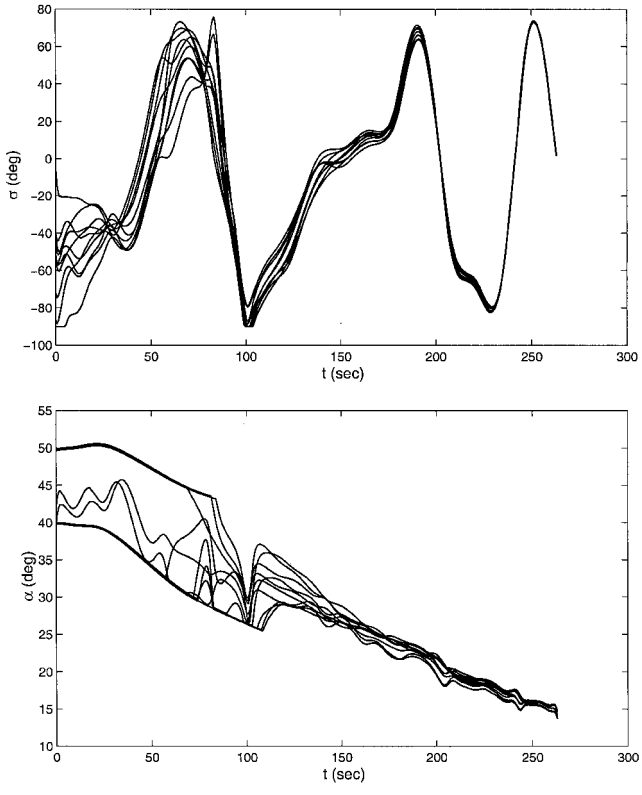

Fig. 7 Variations of dispersed bank angle and angle of attack.

some other monotonic variable (e.g., energy) as the independent variable in defining the reference trajectory is deemed to be more advantageous, the methodology has no difficulty in applying to such a case. Note that linearized system relation (32) (A and B matrices in particular) will be different if a different independent variable is used; therefore the control law must be reformulated accordingly.

2) Both the Space Shuttle and the X-33 entry guidance use α modulation for better tracking performance, particularly during bank reversals. Without α compensation, bank reversals tend to degrade the trajectory control accuracy significantly. The current approach provides coordinated and continuous σ and α modulation commands that do not call for sudden changes (reversals).

3) The controllability of linearized dynamics (32) that is required for the trajectory control law to exist is guaranteed by allowing both σ and α as controls (with the variation in $\Delta\alpha$ restricted). With only σ as the control, the linearized dynamics are not controllable at $\sigma = 0$ or $\sigma = \pm 90$ (deg). In such a case the M^T matrix in Eq. (15) will not be full rank; thus the matrix inverses in control law (16) will not exist.

4) The tightness of the trajectory control depends directly on the control margins available, i.e., the allowable sizes of $\Delta\sigma$ and $\Delta\alpha$. The larger the margins are, the higher controller gain (smaller h parameter) may be used for tighter trajectory control, or the larger trajectory dispersions can be accommodated for the same controller gain. When we keep increasing the magnitudes of trajectory dispersions to the point when divergence occurs, it is always inevitably due to control saturations.

5) Some simple tests have also been done on the robustness of the trajectory control law with respect to aerodynamic uncertainties. One of the noted advantages of the receding-horizon control is its robustness. In this entry guidance application, the preliminary finding suggests again that robustness is strongly dependent on the available control margins. With larger margins, more substantial uncertainties can be compensated for by the feedback control law. No effort has been made yet on comparing the robustness of the drag-tracking guidance strategy of the Shuttle/X-33 and the current method. But the conjecture is that when the control margins are severely limited, the drag-tracking approach will probably be more robust, because the current approach attempts to regulate all the state variables rather than track just one function of the state.

6) The performance of the control law is very insensitive to the choice of the Q matrix. The choice of the R matrix has a more noticeable effect in balancing the relative magnitudes of $\Delta\sigma$ and $\Delta\alpha$, but is far from highly critical.

7) In recent years other entry guidance strategies have also been proposed. Among them, a predictor–corrector guidance method is investigated in Ref. 11. This scheme integrates the trajectory on board and iterates on the targeting conditions to generate the guidance commands. Approximate feedback linearization is used in Ref. 12 to construct control laws for essentially the magnitude of the lift and bank angle to track a predesigned ground track. The current approach adds to the wealth of the available entry guidance methods. It appears to be well suited for missions in which high precision in several or all the states of the trajectory is critical, and the methodology provides a degree of confidence without necessarily requiring extensive simulations for many cases, because the stability is established theoretically for appropriately selected controller parameters.

IV. Conclusions

In a general context, this paper introduces a method to control nonlinear dynamic systems to follow preplanned time-varying reference trajectories. The approach uses an analytical approximate receding-horizon control law. Its major advantages over conventional gain-scheduled controllers are that the closed-loop stability is theoretically ensured for appropriately chosen controller parameters and the controller gains need not be explicitly recomputed when the reference trajectory is changed.

As a specific application, the entry guidance problem for the X-33 vehicle is revisited to demonstrate the potential of this approach. The entry guidance problem is treated as a trajectory-regulation problem about a nominal time-varying trajectory. Even in the presence of relatively large off-nominal trajectory dispersions, the trajectory is still accurately controlled to achieve the desired state in all six state variables of the three-dimensional motion. In comparison, previous methods have not been able to attain this level of overall precision. This application provides a strong support to the proposed approach as a promising candidate for trajectory control and guidance in missions where high precision is critical.

Appendix: Expressions of H and S Matrices

In Eq. (13) the sizes and expressions of H and S depend on the value of N [the term q in Eq. (13) does not affect solution (16)]. For an integer N let

$$H = \begin{bmatrix} H_{00} & H_{01} & \cdots & H_{0(N-1)} \\ H_{10} & H_{11} & \cdots & H_{1(N-1)} \\ \vdots & \vdots & \ddots & \vdots \\ H_{(N-1)0} & H_{(N-1)1} & \cdots & H_{(N-1)(N-1)} \end{bmatrix} \tag{A1}$$

and

$$S = [S_0 \quad S_1 \quad \cdots \quad S_{N-1}] \tag{A2}$$

For $N = 2$:

$$H_{00} = hR + 2hG_{1,0}^T QG_{1,0} + hG_{2,0}^T QG_{2,0}$$

$$H_{11} = 2hR + hG_{2,1}^T QG_{2,1}$$

$$H_{01} = H_{10} = hG_{2,0}^T QG_{2,1}$$

$$S_0 = 2h\Delta_1^T QG_{1,0} + h\Delta_2^T QG_{2,0}$$

$$S_1 = h\Delta_2^T QG_{2,1} \tag{A3}$$

For $N = 3$:

$$H_{00} = hR + 2hG_{1,0}^T QG_{1,0} + 2hG_{2,0}^T QG_{2,0} + hG_{3,0}^T QG_{3,0}$$
$$H_{11} = 2hR + 2hG_{2,1}^T QG_{2,1} + hG_{3,1}^T QG_{3,1}$$
$$H_{22} = 2hR + hG_{3,2}^T QG_{3,2}$$
$$H_{01} = H_{10} = 2hG_{2,0}^T QG_{2,1} + hG_{3,0}^T QG_{3,1}$$
$$H_{02} = H_{20} = hG_{3,0}^T QG_{3,2}$$
$$H_{12} = H_{21} = hG_{3,1}^T QG_{3,2}$$
$$S_0 = 2h\Delta_1^T QG_{1,0} + 2h\Delta_2^T QG_{2,0} + h\Delta_3^T QG_{3,0}$$
$$S_1 = 2h\Delta_2^T QG_{2,1} + h\Delta_3^T QG_{3,1}$$
$$S_2 = h\Delta_3^T QG_{3,2} \tag{A4}$$

For $N = 4$:

$$H_{00} = hR + 2hG_{1,0}^T QG_{1,0} + 2hG_{2,0}^T QG_{2,0} + 2hG_{3,0}^T QG_{3,0} + hG_{4,0}^T QG_{4,0}$$
$$H_{11} = 2hR + 2hG_{2,1}^T QG_{2,1} + 2hG_{3,1}^T QG_{3,1} + hG_{4,1}^T QG_{4,1}$$
$$H_{22} = 2hR + 2hG_{3,2}^T QG_{3,2} + hG_{4,2} QG_{4,2}$$
$$H_{33} = 2hR + hG_{4,3}^T QG_{4,3}$$
$$H_{01} = H_{10} = 2hG_{2,0}^T QG_{2,1} + 2hG_{3,0}^T QG_{3,1} + hG_{4,0}^T QG_{4,1}$$
$$H_{02} = H_{20} = 2hG_{3,0}^T QG_{3,2} + hG_{4,0}^T QG_{4,2}$$
$$H_{03} = H_{30} = hG_{4,0}^T QG_{4,3}$$
$$H_{12} = H_{21} = hG_{3,1}^T QG_{3,2}$$
$$H_{13} = H_{31} = hG_{4,1}^T QG_{4,3}$$
$$H_{23} = H_{32} = hG_{4,2}^T QG_{4,3}$$
$$S_0 = 2h\Delta_1^T QG_{1,0} + 2h\Delta_2^T QG_{2,0} + 2h\Delta_3^T QG_{3,0} + h\Delta_4^T QG_{4,0}$$
$$S_1 = 2h\Delta_2^T QG_{2,1} + 2h\Delta_3^T QG_{3,1} + h\Delta_4^T QG_{4,1}$$
$$S_2 = 2h\Delta_3^T QG_{3,2} + h\Delta_4^T QG_{4,2}$$
$$S_3 = h\Delta_4^T QG_{4,3} \tag{A5}$$

For other values of N, it is not difficult to follow the patterns exhibited in the preceding expressions and obtain the corresponding H and S matrices.

Acknowledgments

This research was supported in part by the NASA Marshall Space Flight Center under Grant NAG8-1289 with John Hanson as the technical monitor. The author thanks Lijun Tian for the help on implementation of the algorithms in MATLAB®.

References

[1]Harpold, J. C., and Graves, C. A., "Shuttle Entry Guidance," *The Journal of the Astronautical Sciences*, Vol. 37, No. 3, 1979, pp. 239–268.

[2]Dukeman, G. A., and Gallaher, M. W., "Guidance and Control Concepts for the X-33 Technology Demonstrator," *21st Annual AAS Guidance and Control Conference*, Paper AAS-98-026, American Astronomical Society, Washington, DC, 1998.

[3]Lu, P., and Hanson, J., "Entry Guidance for the X-33 Vehicle," *Journal of Spacecraft and Rockets*, Vol. 35, No. 3, 1998, pp. 342–349.

[4]Lu, P., Hanson, J., Dukeman, G., and Bhargav, S., "An Alternative Entry Guidance Scheme for the X-33 Vehicle," *Proceedings of the AIAA Atmospheric Flight Mechanics Conference*, AIAA, Reston, VA, 1998, pp. 283–292.

[5]Roenneke, A. J., and Markl, A., "Reentry Control of a Drag Versus Energy Profile," *Journal of Guidance, Control, and Dynamics*, Vol. 17, No. 5, 1994, pp. 916–920.

[6]Lu, P. "Analytical Control Laws for Linear Time-Varying Systems via an Approximate Receding-Horizon Control Approach," *IEEE Transactions on Automatic Control* (to be published).

[7]Chen, C. T., *Linear System Theory and Design*, CBS College Publishing, New York, 1984, pp. 182–183.

[8]Kwon, W. H., and Pearson, A. E., "A Modified Quadratic Cost Problem and Feedback Stabilization of a Linear System," *IEEE Transactions on Automatic Control*, Vol. 22, No. 5, 1977, pp. 838–842.

[9]Vinh, N. X., Busemann, A., and Culp, R. D., *Hypersonic and Planetary Entry Flight Mechanics*, Univ. of Michigan Press, Ann Arbor, MI, 1980, pp. 26, 27.

[10]Zhou, J. L., Tits, A. L., and Lawrence, C. T., "User's Guide for FFSQP Version 3.7: A FORTRAN Code for Solving Constrained Nonlinear (Minimax) Optimization Problems, Generating Iterates Satisfying all Inequality and Linear Constraints," Systems Research Center TR-92-107r2, Univ. of Maryland, College Park, MD, April 1997.

[11]Powell, R. W., and Braun, R. D., "Six-Degree-of-Freedom Guidance and Control Analysis of Mars Aerocapture," *Journal of Guidance, Control, and Dynamics*, Vol. 16, No. 6, 1993, pp. 1038–1044.

[12]Bharadwaj, S., Rao, A. V., and Mease, K. D., "Entry Trajectory Tracking Law via Feedback Linearization," *Journal of Guidance, Control, and Dynamics*, Vol. 21, No. 5, 1998, pp. 726–732.